On the role of four-wave mixing effect in the interactions between nonlinear modes of coupled generalized nonlinear Schrödinger equation

N. Vishnu Priya,[1,a)] M. Senthilvelan,[2,b)] (iD) and Govindan Rangarajan[1,c)]

AFFILIATIONS

[1] Department of Mathematics, Indian Institute of Science, Bengaluru 560 012, Karnataka, India
[2] Department of Nonlinear Dynamics, Bharathidasan University, Tiruchirappalli 620 024, Tamil Nadu, India

[a)] **Electronic mail:** vishnupriyan@iisc.ac.in
[b)] **Electronic mail:** velan@cnld.bdu.ac.in
[c)] **Electronic mail:** rangaraj@iisc.ac.in

ABSTRACT

In this paper, we investigate the effect of four-wave mixing in the interactions among nonlinear waves such as solitons, breathers, and rogue waves of a coupled generalized nonlinear Schrödinger equation. We explore several interesting results including superposition of breather pulses, increment in the number of breather pulses and in amplitudes of breathers, and rogue waves. By strengthening the four-wave mixing parameter, we observe different transformations that occur between different localized structures. For instance, we visualize a transformation from bright soliton to breather form, bright and dark rogue wave to four-petaled rogue wave structures, four-petaled rogue wave to other rogue wave forms, and so on. Another important observation that we report here is that the interaction of a bright soliton with a rogue wave in the presence of the four-wave mixing effect provides interaction between a dark oscillatory soliton and a rogue wave.

Published under license by AIP Publishing. https://doi.org/10.1063/1.5121245

Studies on nonlinear waves are of contemporary interest in several areas of science. The outcome helps us to understand the behavior of real water waves, wave transmission in optical fibers, gas dynamics, DNA, black holes, and so on. These waves are modeled by nonlinear partial differential equations (PDEs). The nonlinear Schrödinger (NLS) equation is a prototypical PDE, which describes the evolution of slowly varying wave packets in various physical systems. The exact solutions of the NLS equation have brought out several interesting nonlinear wave phenomena such as solitons, breathers, and rogue waves. Recently, the interaction between these nonlinear localized waves has been explored for a hierarchy of NLS equation. In this paper, we investigate these interactions in a coupled generalized NLS equation. In particular, we study how the four-wave mixing parameter affects the interactions between nonlinear waves by constructing exact analytical expressions. Since the four-wave mixing effect has fundamental importance in nonlinear optics, we hope that our results will be useful in nonlinear optical fiber experiments.

I. INTRODUCTION

One of the important physical models that describe the evolution of slowly varying wave packets in various nonlinear systems is the nonlinear Schrödinger (NLS) equation.[1,2] The localized solutions of the NLS equation, namely, solitons, breathers, and rogue waves, have many potential applications in different areas of physics including light wave technology, plasma physics, water waves, photonics, nonlinear optics, optical waveguide arrays, and in condensed matter physics.[3–8] A soliton is a localized wave that arises from the balance between nonlinear and dispersive effects.[9] It maintains its shape when it propagates at a constant velocity. The breather solution of the NLS equation is a localized wave with a temporally and/or spatially periodic structure having a constant background exhibiting internal oscillations and bound states of nonlinear wave packets.[10] A rogue wave models extreme events that occur in the ocean, which are localized in both space and time.[9] Interestingly, several integrable generalizations of the NLS equation also exhibit these localized structures (see, for example, Refs. 11–19).

In a variety of complex nonlinear systems, several amplitudes rather than a single one need to be considered. The resulting system of coupled NLS equations describes the wave dynamics with higher accuracy than the scalar NLS equation. Studies in this direction show that coupled NLS equations admit several novel localized structures including bright-bright, dark-dark, bright-dark solitons, vector breather, and vector rogue waves (see, for example, Refs. [20]–[35]). During the past ten years, several works have been devoted to investigating the interaction properties and their mechanisms of the aforementioned localized nonlinear waves in certain coupled systems. Their interaction properties have led to many interesting applications. For example, a vector bright soliton can be used to generate a Bell state in ultracold atoms,[36] bright soliton interferometry,[37] and so on.

In this paper, we consider the following coupled generalized nonlinear Schrödinger (CGNLS) equation:

$$ip_t + p_{xx} + 2(a|p|^2 + c|q|^2 + bpq^* + b^*qp^*)p = 0,$$
$$iq_t + q_{xx} + 2(a|p|^2 + c|q|^2 + bpq^* + b^*qp^*)q = 0,$$
(1)

where p and q are slowly varying pulse envelopes and a and c are real constants corresponding to self-phase modulation and cross phase modulation effects, respectively. Here, b is a complex constant corresponding to four-wave mixing and $*$ denotes complex conjugation. Besides self-phase and cross phase modulation effects, four-wave mixing effects have also been included in (1). When $a = c$ and $b = 0$, the above equation reduces to the Manakov system.[20] When $a = -c$ and $b = 0$, it reduces to the mixed coupled nonlinear Schrödinger equation.[38] Painlevé analysis carried out on system (1) reveals that it is an integrable equation for arbitrary values of the system parameters a, b, and c.[39] Equation (1) admits a Lax pair and an infinite number of conservation laws.[40] In Ref. [40], the authors have derived an N-bright-bright soliton formula for system (1) with a restriction on the system parameters a, b, and c.

Two of the present authors have derived N-bright-bright soliton and N-dark-dark soliton solutions of (1) without any parametric restriction on the system parameters (a, b, and c) in Ref. [41]. We have also constructed general breather, Akhmediev breather, Ma soliton and rogue wave solutions of (1) using the Hirota bilinearization method and studied the effect of four-wave mixing in these solutions.[42] Further, we have presented a higher order and Nth order rogue wave solutions of (1) with the help of modified and generalized Darboux transformation (DT) methods, respectively, in Refs. [43] and [44]. A connection between rogue wave and modulation instability through four-wave mixing parameter has been reported in Ref. [45].

To derive dark soliton, breather, and rogue wave solutions through the DT method, one should choose a plane wave solution as the seed solution, that is,

$$p[0] = \tau_1 e^{i(k_1 x + \omega_1 t)}, \quad q[0] = \tau_2 e^{i(k_2 x + \omega_2 t)},$$
(2)

where τ_1, τ_2, k_1, k_2, ω_1, and ω_2 are real constants, for this equation. It is clear that the presence of four-wave mixing parameters b and b^* restricts us to obtain a dispersion relation with $k_1 \neq k_2$. In order to obtain a consistent dispersion relation, one should choose $k_1 = k_2$. Due to this restriction, both components p and q should

necessarily be described by the same background plane wave solution (the components p and q differ only in amplitude). Hence, the dark solitons, breather, and rogue wave solution constructed earlier by two of the present authors have come up with the same background in both components.[42] Very recently, Mukam et al. have studied certain interaction properties, namely, soliton-rogue wave and breather-rogue wave interactions in this model.[46] The authors have investigated the aforementioned interactions with the same background in the seed solutions (which differ only in amplitudes) for both components p and q. To the authors' knowledge, how the four-wave mixing parameter influences the interaction has not been reported so far.

However, recently, Agalarov et al. have overcome this restriction by introducing a transformation,[47]

$$p = \psi_1 - b^*\psi_2, \quad q = a\psi_2,$$
(3)

in (1), so that Eq. (1) becomes

$$i\psi_{1t} + \psi_{1xx} + 2a(|\psi_1|^2 + \sigma|\psi_2|^2)\psi_1 = 0,$$
$$i\psi_{2t} + \psi_{2xx} + 2a(|\psi_1|^2 + \sigma|\psi_2|^2)\psi_2 = 0,$$
(4)

where $\sigma = ac - |b|^2$. In the case $a = \sigma = 1$, Eq. (4) becomes the basic Manakov model. One can observe that the four-wave mixing term is implicitly defined in Eq. (4). The advantage of transforming the CGNLS equation into (4) is that in the latter equation, one can construct dark soliton, breather, and rogue wave solution with two different background seed solutions. With this reduction procedure, Agalarov et al. have constructed bright-bright soliton solution for both focusing and defocusing regimes. They have also constructed dark-dark soliton with two different background plane wave solutions. In addition, they have derived quasibreather and dark soliton solutions for model (1). By following their work, recently, N-bright-dark soliton solution for Eq. (1) has been constructed in Ref. [48]. Very recently, Yuan et al. have studied the interactions between various nonlinear modes in model (1).[49] However, the authors have again opted for the same background for the seed solutions for both components ψ_1 and ψ_2. As a result, they have obtained similar results as presented in Ref. [46].

As we pointed out earlier, a thorough investigation on the interaction among various modes may lead to new potential applications. As far as the CGNLS equation is concerned, the interaction properties of various localized modes with two different backgrounds are yet to be studied in detail. Four-wave mixing is a basic nonlinear phenomenon having fundamental relevance and practical applications in several areas of physics, in particular, nonlinear optics,[50] optical processing,[51] phase conjugate optics,[52] real time holography,[53] measurement of atomic energy structures, and decay rates,[54] to name a few. In this paper, we intend to study how the four-wave mixing parameter b influences the interaction picture between a soliton, breather, and rogue wave of CGNLS system (1) with two different background seed solutions. Our investigations reveal that the four-wave mixing parameter makes the following changes in interaction picture between localized waves: (i) it turns a bright soliton into a breather form, (ii) it increases the number of pulses of the breather, (iii) it increases the amplitude of the breather, (iv) it decreases the depth of the dark soliton in a dark soliton-breather interaction, (v) in a bright soliton-rogue wave interaction, it changes

the bright soliton into the dark oscillating soliton, (vi) in a dark soliton-rogue wave interaction, it increases the depth of the dark soliton and the amplitude of the rogue wave, (vii) it gives superposition of breather pulses, (viii) it changes both a rogue wave and a dark rogue wave into four-petaled rogue waves, (ix) it exhibits double rogue waves on the oscillating background, and (x) as the rogue wave turns into a four-petaled rogue wave, it changes a four-petaled rogue wave into a classical rogue wave.

We organize our presentation as follows. In Sec. II, we present the DT method and construct nonlinear wave solutions to CGNLS system (1). We give three different families of nonlinear wave solutions to the CGNLS system in Sec. III. We also study the effect of four-wave mixing in three generic cases. In particular, we investigate in detail how the four-wave mixing parameter influences the interactions between nonlinear waves such as bright soliton, dark soliton, breather, and rogue waves. Our results reveal that the interactions exhibit the aforementioned properties. We present our conclusions in Sec. IV.

II. DARBOUX TRANSFORMATION OF THE CGNLS SYSTEM

In our study, we consider only the focusing case of a coupled NLS system (4), that is, $a, \sigma > 0$. The Lax pair or eigenvalue problem of Eq. (4) is given by

$$\Phi_x = U\Phi = (J\lambda + \Psi)\Phi,$$
$$\Phi_t = V\Phi = (J\lambda^2 + \Psi\lambda + V_0)\Phi, \qquad (5)$$

with

$$J = \begin{pmatrix} \dfrac{-2i}{3} & 0 & 0 \\ 0 & \dfrac{i}{3} & 0 \\ 0 & 0 & \dfrac{i}{3} \end{pmatrix}, \quad \Psi = \begin{pmatrix} 0 & \sqrt{a}\psi_1 & \sqrt{a\sigma}\psi_2 \\ -\sqrt{a}\psi_1^* & 0 & 0 \\ -\sqrt{a\sigma}\psi_2^* & 0 & 0 \end{pmatrix}, \qquad (6)$$

and

$$V_0 = \begin{pmatrix} ia|\psi_1|^2 + ia\sigma|\psi_2|^2 & i\sqrt{a}\psi_{1t} & i\sqrt{a\sigma}\psi_{2t} \\ i\sqrt{a}\psi_{1t}^* & -ia|\psi_1|^2 & -ia\sqrt{\sigma}\psi_2\psi_1^* \\ i\sqrt{a\sigma}\psi_{2t}^* & -ia\sqrt{\sigma}\psi_2^*\psi_1 & -ia\sqrt{a\sigma}|\psi_2|^2 \end{pmatrix}, \quad (7)$$

where λ is a complex spectral parameter and $\Phi(x, t, \lambda)$ is the three component vector. Equation (4) can be obtained from the zero curvature condition $U_t - V_x + [U, V] = 0$, where the square bracket denotes the usual commutator.

The DT for coupled NLS equation (4) has already been presented in the literature.[24,55] Avoiding those details here, we write only the end result of it. Considering Φ at $\lambda = \lambda_1$ such as $\Phi_1 = (\phi_1(x, t, \lambda_1), \phi_2(x, t, \lambda_1), \phi_3(x, t, \lambda_1))^T$, the first iterated DT solution formula of coupled NLS equation (4) reads[28]

$$\psi_1[1] = \psi_1^{[0]} - \frac{1}{\sqrt{a}} \frac{i(\lambda_1 - \lambda_1^*)\phi_1\phi_2^*}{|\phi_1|^2 + |\phi_2|^2 + |\phi_3|^2},$$
$$\psi_2[1] = \psi_2^{[0]} - \frac{1}{\sqrt{a\sigma}} \frac{i(\lambda_1 - \lambda_1^*)\phi_1\phi_3^*}{|\phi_1|^2 + |\phi_2|^2 + |\phi_3|^2}. \qquad (8)$$

Substituting the expressions ϕ_1, ϕ_2, and ϕ_3 into (8) yields the forms $\psi_1[1]$ and $\psi_2[1]$. Plugging the explicit forms of $\psi_1[1]$ and $\psi_2[1]$ in the transformation given in (3), we can obtain the first iterated solution of CGNLS system (1) in the form

$$p[1] = \left(\psi_1^{[0]} - \frac{1}{\sqrt{a}} \frac{i(\lambda_1 - \lambda_1^*)\phi_1\phi_2^*}{|\phi_1|^2 + |\phi_2|^2 + |\phi_3|^2}\right)$$
$$- b^*\left(\psi_2^{[0]} - \frac{1}{\sqrt{a\sigma}} \frac{i(\lambda_1 - \lambda_1^*)\phi_1\phi_3^*}{|\phi_1|^2 + |\phi_2|^2 + |\phi_3|^2}\right), \qquad (9)$$
$$q[1] = a\left(\psi_2^{[0]} - \frac{1}{\sqrt{a\sigma}} \frac{i(\lambda_1 - \lambda_1^*)\phi_1\phi_3^*}{|\phi_1|^2 + |\phi_2|^2 + |\phi_3|^2}\right).$$

We can construct the desired solution of (1) through Eq. (9) by appropriately choosing the seed solutions and solving the respective Lax pair equation and then substituting the obtained expressions (ϕ_1, ϕ_2, and ϕ_3) in (9).

III. NONLINEAR WAVE SOLUTIONS OF CGNLS SYSTEM

In this section, we construct three different nonlinear wave solutions of (1). To begin, we consider two different plane wave solutions, $\psi_1 = \tau_1 e^{i(k_1 x + \omega_1 t)}$ and $\psi_2 = \tau_2 e^{i(k_2 x + \omega_2 t)}$, as seed solutions of Eq. (4). Substituting these seed solutions into (4), we obtain the following dispersion relations, namely,

$$\omega_1 = 2a\tau_1^2 + 2a\sigma\tau_2^2 - k_1^2, \quad \omega_2 = 2a\tau_1^2 + 2a\sigma\tau_2^2 - k_2^2. \qquad (10)$$

To integrate Lax pair equation (5) with the above seed solutions, we rewrite Eq. (5) in its component form, which yields the following six coupled first order linear ordinary differential equations (ODEs), namely,

$$\phi_{1x} = -\frac{2i}{3}\lambda_1\phi_1 + \sqrt{a}\psi_1\phi_2 + \sqrt{a\sigma}\psi_2\phi_3, \qquad (11a)$$

$$\phi_{2x} = -\sqrt{a}\psi_1^*\phi_1 + \frac{i}{3}\lambda_1\phi_2, \qquad (11b)$$

$$\phi_{3x} = -\sqrt{a\sigma}\psi_2^*\phi_1 + \frac{i}{3}\lambda_1\phi_3, \qquad (11c)$$

$$\phi_{1t} = \left(-\frac{2i}{3}\lambda_1^2 + ia|\psi_1|^2 + ia\sigma|\psi_2|^2\right)\phi_1 + (i\sqrt{a}\psi_{1t}$$
$$+ \sqrt{a}\psi_1\lambda_1)\phi_2 + (\sqrt{a\sigma}\psi_2\lambda_1 + i\sqrt{a\sigma}\psi_{2t})\phi_3, \qquad (11d)$$

$$\phi_{2t} = (i\sqrt{a}\psi_{1t}^* - \sqrt{a}\psi_1^*\lambda_1)\phi_1 + \left(\frac{i}{3}\lambda_1^2 - ia|\psi_1|^2\right)\phi_2$$
$$- ia\sqrt{\sigma}\psi_2\psi_1^*\phi_3, \qquad (11e)$$

$$\phi_{3t} = (-\sqrt{a\sigma}\psi_2^*\lambda_1 + i\sqrt{a\sigma}\psi_{2t}^*)\phi_1 - ia\sqrt{\sigma}\psi_2^*\psi_1\phi_2$$
$$+ \left(\frac{i}{3}\lambda_1^2 - ia\sigma|\psi_2|^2\right)\phi_3. \qquad (11f)$$

Substituting the assumed seed solutions in (11) and integrating the resultant set of ODEs, we can get the eigenfunctions $\Phi_1 = (\phi_1, \phi_2, \phi_3)$.

Since the method of solving the set of Eqs. (11) is rather lengthy and tedious, in the following, we present only the outline of it. To

begin, we consider the first three equations, (11a)–(11c), which are associated with the spatial part. We rewrite these three first order ODEs as a single third order linear ODE in $\phi_1(x,t)$ and its derivatives. We integrate this third order ODE and obtain the explicit form

of $\phi_1(x,t)$ from which we derive the exact expressions of $\phi_2(x,t)$ and $\phi_3(x,t)$. We substitute back these expressions in the remaining three equations, (11d)–(11f), and integrate them to obtain the time dependent part in them.

The general solution of the third order ODE for $\phi_1(x,t)$ that comes out from the spatial part can be fixed by solving the following characteristic polynomial equation,[28] namely,

$$m^3 - i(k_1 + k_2)m^2 + \left(a\tau_1^2 + a\sigma\tau_2^2 + \frac{1}{3}\lambda_1(\lambda_1 + k_1 + k_2) - k_1 k_2\right)m - \left(ia\tau_1^2\left(k_2 + \frac{\lambda_1}{3}\right) + ia\sigma\tau_2^2\left(k_1 + \frac{\lambda_1}{3}\right)\right)$$

$$+ \frac{2i}{3}\lambda_1\left(\frac{\lambda_1^2}{9} + \frac{\lambda_1}{3}(k_1 + k_2) + k_1 k_2\right)\right) = 0. \tag{12}$$

The general form of $\phi_1(x,t)$ depends on the roots of Eq. (12). The cubic polynomial (12) may have (i) three different roots, (ii) one single and one double root, and (iii) three equal roots. The solutions of these three cases bring out to three different families of nonlinear waves of (1). In the following, we consider all three possibilities and report the outcome.

A. Case 1: All three roots are different

In the first case, we consider that all three roots of the characteristic equation (12) are different. Depending on the roots as m_1, m_2, and m_3, we obtain the following expression for ϕ_1, ϕ_2, and ϕ_3, that is,

$$\phi_1 = c_1 \exp\left[\left(m_1 + \frac{i}{3}(k_1 + k_2)\right)x + \left(im_1^2 + \frac{2m_1}{3}(\lambda_1 - k_1 - k_2) + \frac{2i}{9}(\lambda_1^2 + (k_1 + k_2)\lambda_1\right.\right.$$

$$\left. - k_1 k_2) + 2i(a\tau_1^2 + a\sigma\tau_2^2) - \frac{i}{9}(k_1^2 + k_2^2)\right)t\right] + c_2 \exp\left[\left(m_2 + \frac{i}{3}(k_1 + k_2)\right)x\right.$$

$$+ \left(im_2^2 + \frac{2m_2}{3}(\lambda_1 - k_1 - k_2) + \frac{2i}{9}(\lambda_1^2 + (k_1 + k_2)\lambda_1 - k_1 k_2) + 2i(a\tau_1^2 + a\sigma\tau_2^2)\right.$$

$$\left. - \frac{i}{9}(k_1^2 + k_2^2)\right)t\right] + c_3 \exp\left[\left(m_3 + \frac{i}{3}(k_1 + k_2)\right)x + \left(im_3^2 + \frac{2m_3}{3}(\lambda_1 - k_1 - k_2)\right.\right.$$

$$\left.\left. + \frac{2i}{9}(\lambda_1^2 + (k_1 + k_2)\lambda_1 - k_1 k_2) + 2i(a\tau_1^2 + a\sigma\tau_2^2) - \frac{i}{9}(k_1^2 + k_2^2)\right)t\right],$$

$$\phi_2 = \frac{-\sqrt{a}\tau_1}{m_1 - i\frac{\lambda_1}{3} - \frac{i}{3}(2k_1 - k_2)}c_1 \exp\left[\left(m_1 + \frac{i}{3}(k_2 - 2k_1)\right)x + \left(im_1^2 + \frac{2m_1}{3}(\lambda_1 - k_1 - k_2)\right.\right.$$

$$\left.\left. + \frac{2i}{9}(\lambda_1^2 + (k_1 + k_2)\lambda_1 - k_1 k_2) - \frac{i}{9}k_2^2 + \frac{8i}{9}k_1^2\right)t\right] + \frac{-\sqrt{a}\tau_1}{m_2 - i\frac{\lambda_1}{3} - \frac{i}{3}(2k_1 - k_2)}c_2$$

$$\exp\left[\left(m_2 + \frac{i}{3}(k_2 - 2k_1)\right)x + \left(im_2^2 + \frac{2m_2}{3}(\lambda_1 - k_1 - k_2) + \frac{2i}{9}(\lambda_1^2 + (k_1 + k_2)\lambda_1\right.\right.$$

$$\left.\left. - k_1 k_2) - \frac{i}{9}k_2^2 + \frac{8i}{9}k_1^2\right)t\right] + \frac{-\sqrt{a}\tau_1}{m_3 - i\frac{\lambda_1}{3} - \frac{i}{3}(2k_1 - k_2)}c_3 \exp\left[\left(m_3 + \frac{i}{3}(k_2 - 2k_1)\right)x\right.$$

$$\left. + \left(im_3^2 + \frac{2m_3}{3}(\lambda_1 - k_1 - k_2) + \frac{2i}{9}(\lambda_1^2 + (k_1 + k_2)\lambda_1 - k_1 k_2) - \frac{i}{9}k_2^2 + \frac{8i}{9}k_1^2\right)t\right], \tag{13}$$

$$\phi_3 = \frac{-\sqrt{a\sigma}\tau_2}{m_1 - i\frac{\lambda_1}{3} - \frac{i}{3}(2k_2 - k_1)}c_1 \exp\left[\left(m_1 + \frac{i}{3}(k_1 - 2k_2)\right)x + \left(im_1^2 + \frac{2m_1}{3}(\lambda_1 - k_1 - k_2)\right.\right.$$

$$\left.\left. + \frac{2i}{9}(\lambda_1^2 + (k_1 + k_2)\lambda_1 - k_1 k_2) - \frac{i}{9}k_1^2 + \frac{8i}{9}k_2^2\right)t\right] + \frac{-\sqrt{a\sigma}\tau_2}{m_2 - i\frac{\lambda_1}{3} - \frac{i}{3}(2k_2 - k_1)}c_2$$

$$\exp\left[\left(m_2 + \frac{i}{3}(k_1 - 2k_2)\right)x + \left(im_2^2 + \frac{2m_2}{3}(\lambda_1 - k_1 - k_2) + \frac{2i}{9}(\lambda_1^2 + (k_1 + k_2)\lambda_1\right.\right.$$
$$\left. - k_1 k_2) - \frac{i}{9}k_1^2 + \frac{8i}{9}k_2^2\right)t\right] + \frac{-\sqrt{a\sigma}\,\tau_2}{m_3 - i\frac{\lambda_1}{3} - \frac{i}{3}(2k_2 - k_1)}c_3 \exp\left[\left(m_3 + \frac{i}{3}(k_1 - 2k_2)\right)x\right.$$
$$\left. + \left(im_3^2 + \frac{2m_3}{3}(\lambda_1 - k_1 - k_2) + \frac{2i}{9}(\lambda_1^2 + (k_1 + k_2)\lambda_1 - k_1 k_2) - \frac{i}{9}k_1^2 + \frac{8i}{9}k_2^2\right)t\right].$$

Substituting expressions (13) into DT formula (9), we can obtain a generic solution of (1).

1. The effect of four-wave mixing in case 1

Our aim is to investigate how the four-wave mixing parameter influences the interaction properties. However, in the following, we begin our study by considering the case $b \to 0$. We plot the solution with $\tau_1 \to 0$ and $\tau_2 \neq 0$ by choosing $b \to 0$. This choice enforces the seed solution of the p component put nearly equal to zero and the q component has a plane wave solution. For this choice, we obtain a bright soliton reflection by a breather in the $p[1]$ component and dark soliton reflection by a breather in the $q[1]$ component that are shown in Figs. 1(a) and 1(d), respectively. This result coincides with the one obtained in Ref. 28. When we increase the value of four-wave mixing parameter b, the bright soliton in the $p[1]$ component

converts into a breather form and it is reflected by another breather as shown in Fig. 1(b) (we note that in order to maintain the focusing case, that is, $a > 0$ and $\sigma = ac - |b|^2 > 0$, one should increase the values of a and c appropriately. We incorporate this procedure in all three cases unless otherwise mentioned). As far as the $q[1]$ component is concerned, the depth of the dark soliton decreases when we increase the value of four-wave mixing parameter b. This result also coincides with the one presented in Ref. 47. When we increase the value of b further, the number of breather pulses gets increased and the distance between any two breather pulses gets decreased. In one of our earlier works,[42] we have analytically proved that the distance between any two breather pulses depends on four-wave mixing parameter b. The outcome of the present study confirms our earlier result.

Now, we consider the case $\tau_1, \tau_2 \neq 0$, that is, both components p and q have now plane wave solutions as seed solutions. To
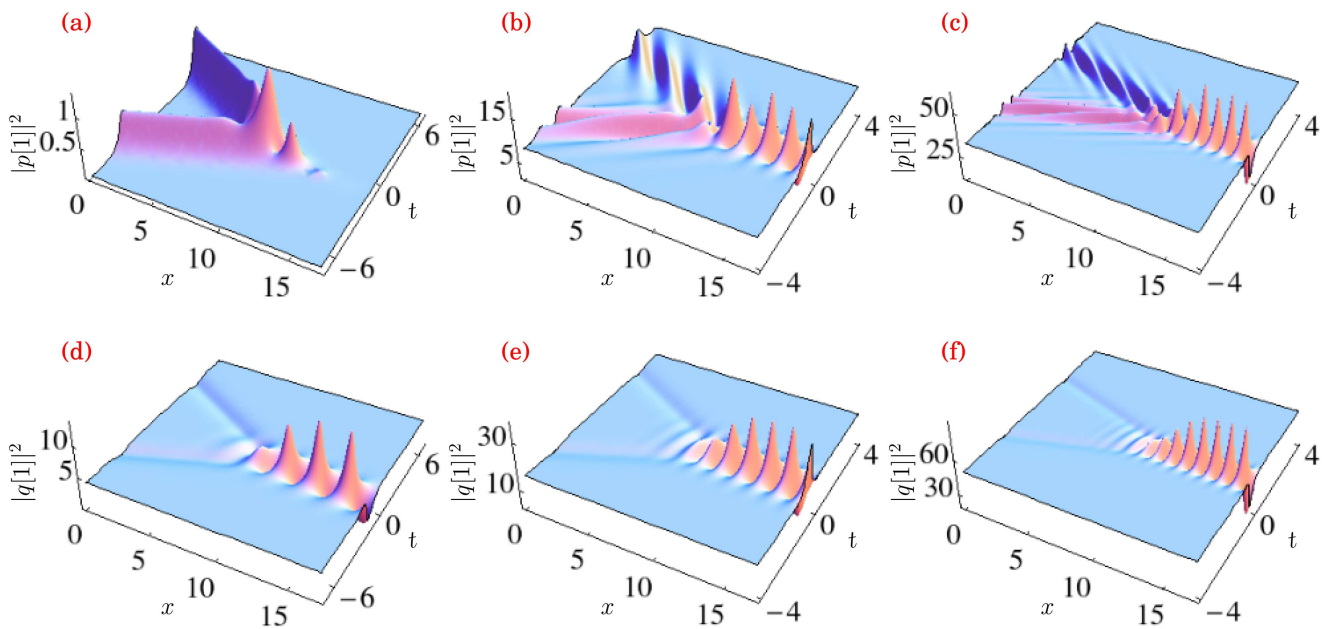
FIG. 1. (a) A bright soliton in one field is reflected like a hard wall by the breather in the other one around $x > 7$ and at $t = 0$. (d) Similarly, a dark soliton is also reflected by the breather for the parameter values $\lambda_1 = 1.2i$, $\tau_1 = 0.001$, $\tau_2 = 2$, $c_1 = 1$, $c_2 = 4$, $c_3 = 3$, $k_1 = -0.5$, $k_2 = 0.5$, $a = 1$, $c = 0.5$, and $b = 0.001 + 0.001i$. (b) The breather is reflected by other breather in $p[1]$ and (e) a dark soliton is reflected by the breather in $q[1]$ for the parameter values $a = 2$, $c = 1.3$, and $b = 1 + i$; the other parameters are the same as above. (c) Number of breather pulses increased in $p[1]$ and (f) the depth of the dark soliton decreased in $q[1]$ for the parameter values $a = 3.5$, $c = 2.5$, and $b = 2 + 2i$; the other parameters are the same as above.

confirm the result of Manakov system, we choose $b \to 0$ and plot the solutions. In this case, we visualize that a breather is reflected by another breather in both components, which is shown in Figs. 2(a) and 2(b). This result is also similar to the one presented in Ref. 28. One may observe that in transformation (3), the component $p[1]$ has been introduced as the superposition of solutions of the Manakov equation components ψ_1 and ψ_2 and the four-wave mixing parameter. As a consequence, when we increase the value of four-wave mixing parameter b in the component $p[1]$, we come across superpositioned breather pulses on the oscillating background as shown in Figs. 2(c) and 2(e). This result is new to the literature as far as the CGNLS equation is concerned. As far as the $q[1]$ component is concerned, we can see the changes only in amplitudes and in the number of pulses of breather, which, in turn, increases when we increase the value of b.

B. Case 2: One single root and one double root

The cubic polynomial equation (12) also admits that a case with two roots are equal and the third root differs from the first one. This happens for a specific condition. To obtain the roots of this case, we consider Eq. (12) in the following form, that is,

$$Am^3 + Bm^2 + Cm + D = 0, \tag{14}$$

with $A = 1$, $B = -i(k_1 + k_2)$, $C = a\tau_1^2 + a\sigma\tau_2^2 + \frac{1}{3}\lambda_1(\lambda_1 + k_1 + k_2) - k_1 k_2$, $D = -(ia\tau_1^2(k_2 + \frac{\lambda_1}{3}) + ia\sigma\tau_2^2(k_1 + \frac{\lambda_1}{3}) + \frac{2i}{3}\lambda_1(\frac{\lambda_1^2}{9} + \frac{\lambda_1}{3}(k_1 + k_2) + k_1 k_2))$. The cubic equation (14) admits one double and one single root provided the coefficients should satisfy the following condition,[56] namely,

$$18ABCD - 4B^3D + B^2C^2 - 4AC^3 - 27A^2D^2 = 0. \tag{15}$$

Substituting the expressions A, B, C, and D and rewriting, it we can obtain an expression for λ_1. Since it is a very lengthy one, we do not present it here. The corresponding roots are given by

$$m_1 = \frac{4ABC - 9A^2D - B^3}{A\Delta}, \quad m_2 = m_3 = \frac{9AD - BC}{2\Delta}, \tag{16}$$

with $\Delta = B^2 - 3AC$. Substituting the relevant expressions in (16), we can obtain the exact value of the roots of m_1 and $m_2 (\equiv m_3)$. Using these roots and the condition given above, we obtain the eigenfunctions in the form

$$\phi_1 = c_1 \exp\left[\left(m_1 + \frac{i}{3}(k_1 + k_2)\right)x + \left(im_1^2 + 2(\lambda_1 - k_1 - k_2)\frac{m_1}{3} + \frac{i}{3}(4a\tau_1^2 + 4a\sigma\tau_2^2 - k_1^2 - k_2^2)\right)t\right]$$
$$+ \left(c_3 x + 2c_3 im_2 t + \frac{2}{3}c_3(\lambda_1 - k_1 - k_2)t + c_2\right)\exp\left[\left(m_2 + \frac{i}{3}(k_1 + k_2)\right)x\right.$$
$$+ \left(im_2^2 + 2(\lambda_1 - k_1 - k_2)\frac{m_2}{3} + \frac{i}{3}(4a\tau_1^2 + 4a\sigma\tau_2^2 - k_1^2 - k_2^2)\right)t\right]$$
$$+ c_3 \exp\left[\left(m_2 + \frac{i}{3}(k_1 + k_2)\right)x + \left(im_2^2 + 2(\lambda_1 - k_1 - k_2)\frac{m_2}{3} + \frac{i}{3}(4a\tau_1^2 + 4a\sigma\tau_2^2 - k_1^2 - k_2^2)\right)t\right],$$

$$\phi_2 = \frac{-\sqrt{a}\tau_1}{m_1 - \frac{i\lambda_1}{3} - \frac{i}{3}(2k_1 - k_2)}c_1 \exp\left[\left(m_1 + \frac{i}{3}(k_2 - 2k_1)\right)x + \left(im_1^2 + 2(\lambda_1 - k_1 - k_2)\frac{m_1}{3}\right.\right.$$
$$+ \frac{i}{3}(-2a\tau_1^2 - 2a\sigma\tau_2^2 - k_2^2 + 2k_1^2)\right)t\right] - \frac{\sqrt{a}\tau_1}{m_2 - \frac{i\lambda_1}{3} - \frac{i}{3}(2k_1 - k_2)}\left(c_3 x + 2ic_3 m_2 t\right.$$
$$+ \frac{2}{3}c_3(\lambda_1 - k_1 - k_2)t + c_2\right)\exp\left[\left(m_2 + \frac{i}{3}(k_2 - 2k_1)\right)x + \left(im_2^2 + 2(\lambda_1 - k_1 - k_2)\frac{m_2}{3}\right.\right.$$
$$+ \frac{i}{3}(-2a\tau_1^2 - 2a\sigma\tau_2^2 - k_2^2 + 2k_1^2)\right)t\right] + \frac{-\sqrt{a}\tau_1 - \frac{\sqrt{a}\tau_1}{m_2 - \frac{i\lambda_1}{3} - \frac{i}{3}(2k_1 - k_2)}}{m_2 - \frac{i\lambda_1}{3} - \frac{i}{3}(2k_1 - k_2)}c_3 \exp\left[\left(m_2\right.\right.$$
$$+ \frac{i}{3}(k_2 - 2k_1)\right)x + \left(im_2^2 + 2(\lambda_1 - k_1 - k_2)\frac{m_2}{3} + \frac{i}{3}(-2a\tau_1^2 - 2a\sigma\tau_2^2 - k_2^2 + 2k_1^2)\right)t\right], \tag{17}$$

$$\phi_3 = \frac{-\sqrt{a\sigma}\tau_2}{m_1 - \frac{i\lambda_1}{3} - \frac{i}{3}(2k_2 - k_1)}c_1 \exp\left[\left(m_1 + \frac{i}{3}(k_1 - 2k_2)\right)x + \left(im_1^2 + 2(\lambda_1 - k_1 - k_2)\frac{m_1}{3}\right.\right.$$
$$+ \frac{i}{3}(-2a\tau_1^2 - 2a\sigma\tau_2^2 - k_1^2 + 2k_2^2)\right)t\right] - \frac{\sqrt{a}\tau_2}{m_2 - \frac{i\lambda_1}{3} - \frac{i}{3}(2k_2 - k_1)}\left(c_3 x + 2ic_3 m_2 t\right.$$

$$+\frac{2}{3}c_3(\lambda_1 - k_1 - k_2)t + c_2\bigg) \exp\bigg[\bigg(m_2 + \frac{i}{3}(k_1 - 2k_2)\bigg)x + \bigg(im_2^2 + 2(\lambda_1 - k_1 - k_2)\frac{m_2}{3}$$

$$+\frac{i}{3}(-2a\tau_1^2 - 2a\sigma\tau_2^2 - k_1^2 + 2k_2^2)\bigg)t\bigg] + \frac{-\sqrt{a\sigma}\,\tau_2 - \frac{\sqrt{a\sigma}\,\tau_2}{m_2 - \frac{i\lambda_1}{3} - \frac{i}{3}(2k_2 - k_1)}}{m_2 - \frac{i\lambda_1}{3} - \frac{i}{3}(2k_2 - k_1)}c_3\exp\bigg[\bigg(m_2$$

$$+\frac{i}{3}(k_1 - 2k_2)\bigg)x + \bigg(im_2^2 + 2(\lambda_1 - k_1 - k_2)\frac{m_2}{3} + \frac{i}{3}(-2a\tau_1^2 - 2a\sigma\tau_2^2 - k_1^2 + 2k_2^2)\bigg)t\bigg].$$

Substituting the above expressions into DT formula (9), we can get a generic solution that describes the breather-rogue wave interaction and the breather-dark rogue wave interaction. In the following, we intend to study the effect of four-wave mixing in these two interactions.

1. The effect of four-wave mixing in case 2

To understand the interplay between a bright soliton with a rogue wave in the $p[1]$ component and a dark soliton with a rogue wave in the $q[1]$ component, we consider $\tau_1 \to 0$, $\tau_2 \neq 0$, and $b \to 0$. To plot solution (9) with expression (17), first we should evaluate
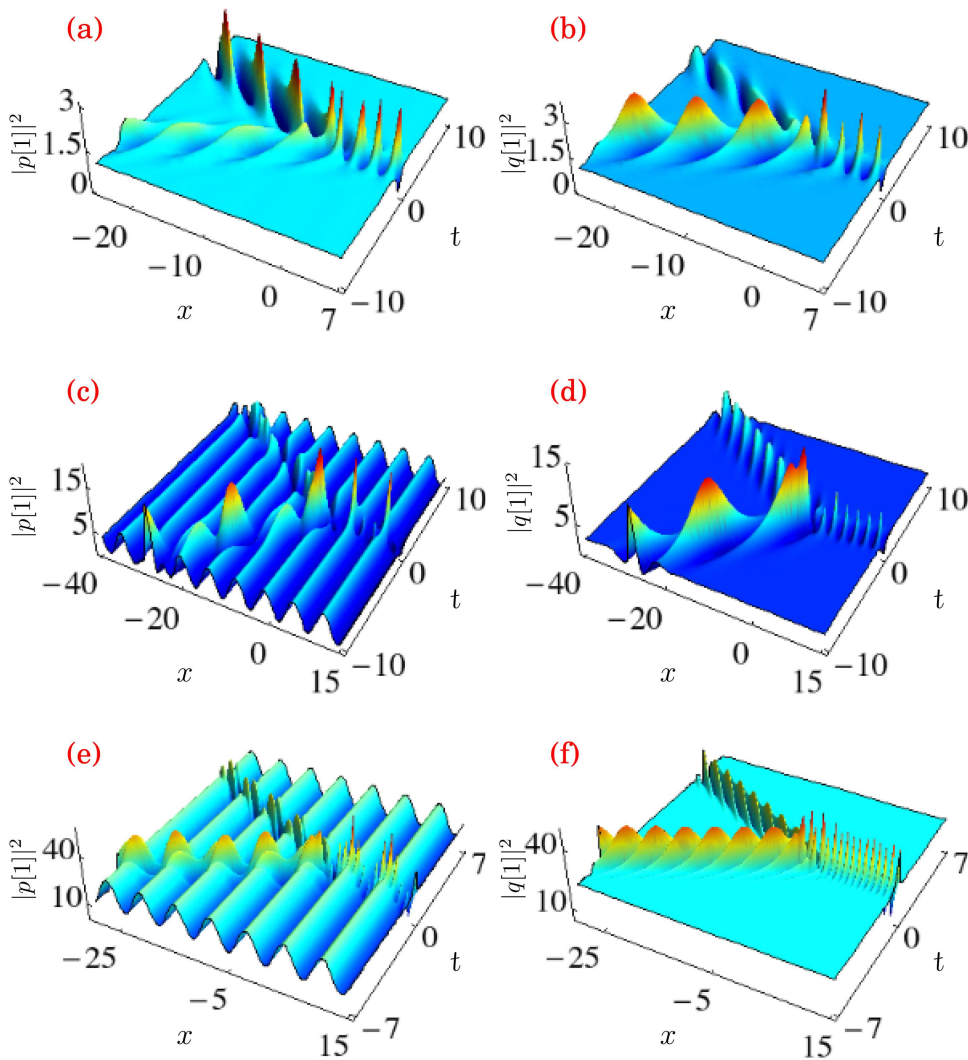
FIG. 2. The breather is reflected by another breather in both (a) $p[1]$ and (b) $q[1]$ components for the parameter values $\tau_1 = 1$, $\tau_2 = 1$, $a = 1$, $c = 1$, and $b = 0.001 + 0.001i$; the other parameters are the same as in Fig. 1. (c) Superposition of breather pulses in $p[1]$ on oscillating background and (d) increasing in amplitude in $q[1]$ for the parameter values $a = 1.5$, $c = 1.5$, and $b = 1 + i$; the other parameters are the same as above. (e) Superposition of breather pulses for the $p[1]$ component and (f) increasing in amplitude in $q[1]$ for the parameter values $a = 4.7$, $c = 4$, and $b = 3 + 3i$; the other parameters are the same as above.
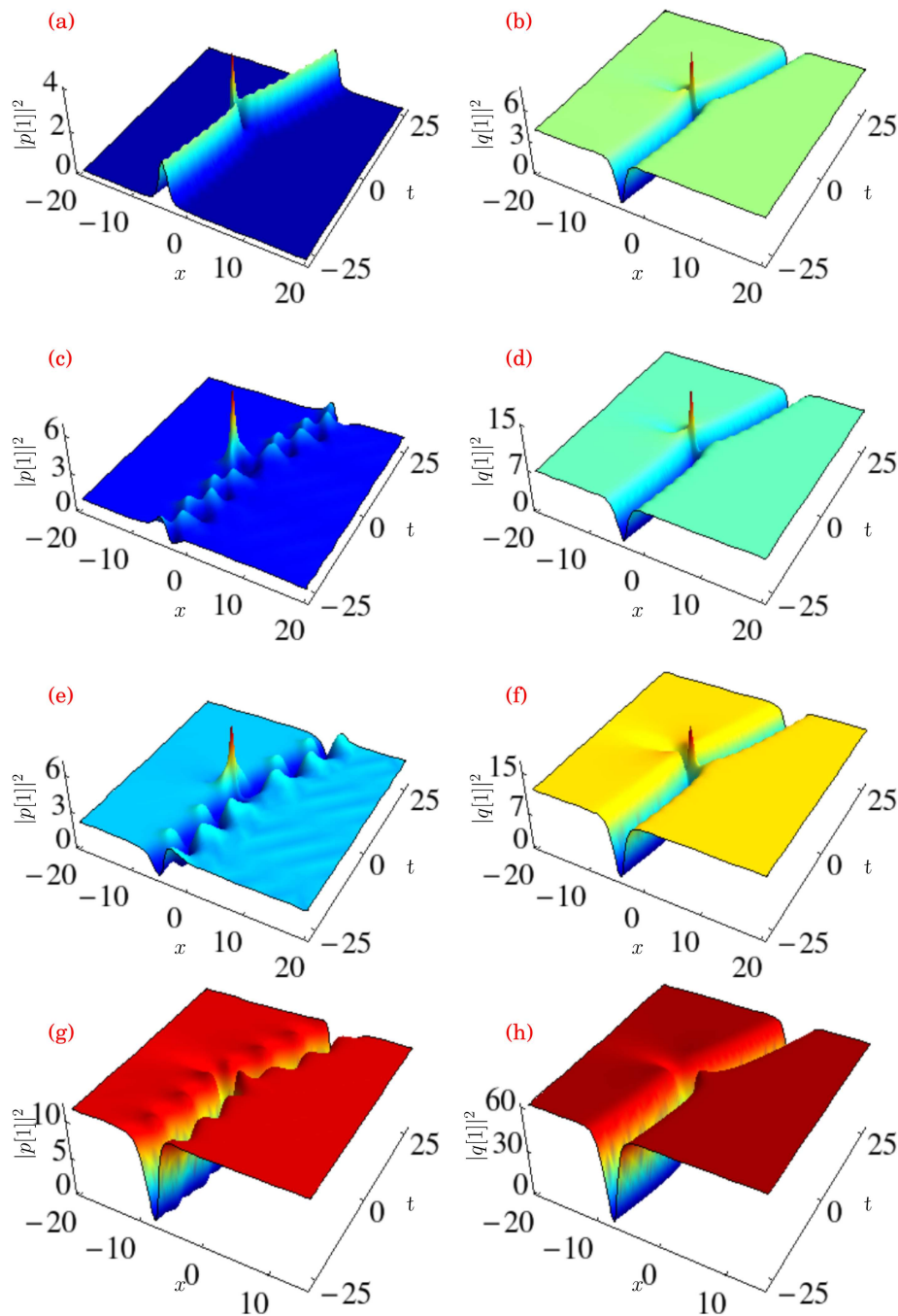
FIG. 3. (a) Bright soliton collision with rogue wave in $p[1]$ and (b) dark soliton collision with rogue wave in $q[1]$ for the parameter values $\lambda_1 = -0.099\,999\,5 - 1.999\,99i$, $\tau_1 = 0.001$, $\tau_2 = 2$, $c_1 = 1$, $c_2 = 4$, $c_3 = 3$, $k_1 = -1$, $k_2 = 0.1$, $a = 1$, $c = 0.25$, and $b = 0.001 - 0.001i$. (c) Bright soliton gets breatherlike form in $p[1]$ and (d) rogue wave amplitude increases in $q[1]$ for the parameter values $\lambda_1 = -0.099\,999\,3 - 1.736\,66i$, $a = 1.3$, $c = 0.25$, and $b = 0.3 - 0.3i$; the other parameters are the same as above. (e) Superposition of the dark soliton with the bright soliton in $|p[1]|$ and (f) rogue wave amplitude increases in $q[1]$ for the parameter values $\lambda_1 = -0.099\,999 - 1.607\,48i$, $a = 1.7$, $c = 0.35$, and $b = 0.5 - 0.5i$; the other parameters are the same as above. (g) Dark oscillating soliton in $p[1]$ and (h) rogue wave amplitude increases in $q[1]$ for the parameter values $\lambda_1 = -0.099\,997\,8 - 1.675\,71i$, $a = 3.9$, $c = 0.75$, and $b = 1.2 - 1.2i$; the other parameters are the same as above.

the exact value of λ_1 from the condition (15) by substituting the other parameter values in it. We present the outcome in Figs. 3(a) and 3(b). To see the influence of the four-wave mixing parameter, we increase the value of b. When $b = 0.3 - 0.3i$, the bright soliton in the $p[1]$ component takes a breatherlike form. By increasing the value of b further, say, for example, $b = 0.5 - 0.5i$ and $b = 1.2 - 1.2i$, we observe that a breatherlike form converts into a dark oscillating

soliton as shown in Fig. 3. This in turn confirms that four-wave mixing can be used to convert the bright soliton into the dark soliton. As far as the $q[1]$ component is concerned, from Fig. 3, we observe that in contrast to case 1, that is, the dark soliton-breather interaction case, the depth of the dark soliton increases with higher values of b. Moreover, the amplitude of rogue wave also increases for higher values of four-wave mixing parameter b.
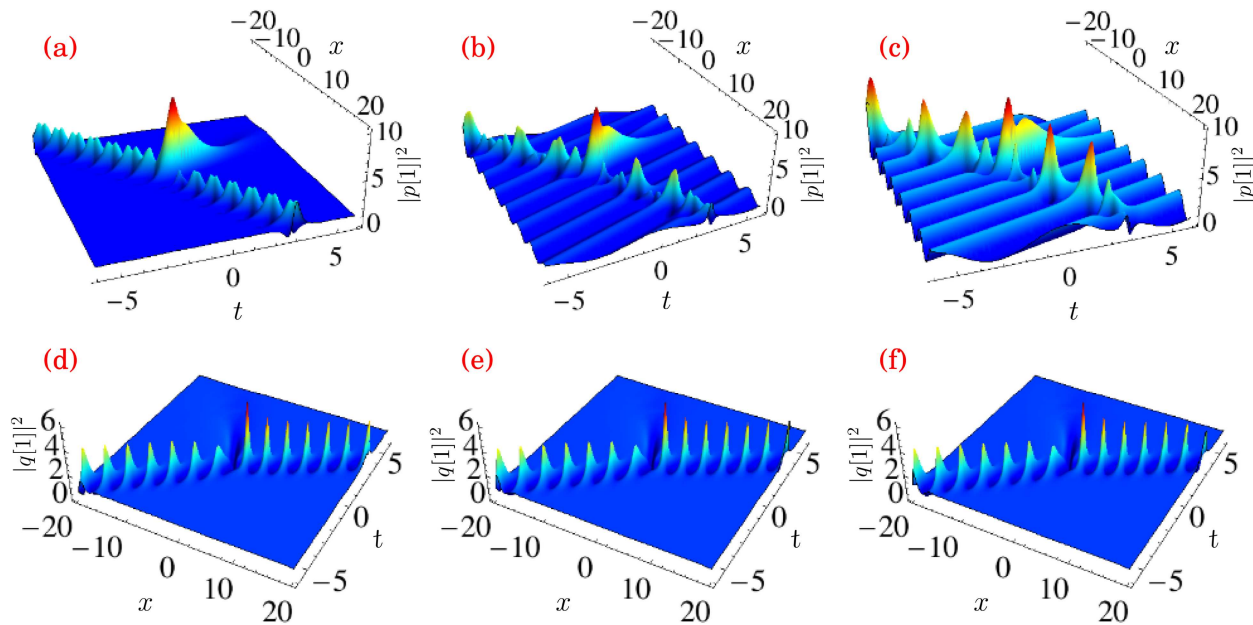
FIG. 4. (a) The breather-rogue wave interaction in $p[1]$ and (d) the breather-dark rogue wave interaction in $q[1]$ for the parameter values $\lambda_1 = -0.276\,068 + 2.144\,98i$, $\tau_1 = 1$, $\tau_2 = 2$, $a = 0.5$, $c = 1.7$, and $b = 0.001 - 0.001i$; the other parameters are as in Fig. 3. (b) Superposition of the breather pulse in $p[1]$ and (e) the breather-dark rogue wave interaction in $q[1]$ for the parameter values $\lambda_1 = -0.242\,524 + 2.129\,24i$, and $b = 0.1 - 0.1i$; the other parameters are the same as above. (c) Superposition of the rogue wave in $p[1]$ and (f) the breather-dark rogue wave interaction in $q[1]$ for the parameter values $\lambda_1 = -0.225\,785 + 2.121\,33i, c = 1.8$, and $b = 0.2 - 0.2i$; the other parameters are the same as above.

Next, we consider the case $\tau_1 \neq 0$, $\tau_2 \neq 0$. To begin, we impose the value of four-wave mixing parameter $b \to 0$. This choice gives the Manakov equation result. In this case, we observe the interactions between breather and rogue wave in the $p[1]$ component and breather and dark rogue wave in the $q[1]$ component. This result coincides with the one presented in Ref. 28. We then move on to analyze the effect of four-wave mixing. As in the previous case, when we increase the value of b, we come across the superposition of breather pulses, as in case 1 [see Fig. 4(b)], and we can see the changes in the rogue wave from Fig. 4(c). To observe the effect of four-wave mixing in rogue wave, we restrict the parameters c_2 and c_3 as $c_2 = c_3 = 0$. With these restrictions, the breather form vanishes and we have only the bright rogue wave in the $p[1]$ component and dark rogue wave in the $q[1]$ component as seen from Figs. 5(a) and 5(d). When we increase the value of b, dark rogue wave in the $q[1]$ component becomes four-petaled rogue wave or antieye shape rogue wave as shown in Fig. 5(e) and 5(f). Due to the superposition expression (3), the component $p[1]$ also exhibits four-petaled rogue wave on the oscillating background for higher values of b, which is shown in Figs. 5(b) and 5(c). From these observations, we conclude that the four-wave mixing effect transforms rogue wave and dark rogue wave into four-petaled rogue wave.

C. Case 3: All three roots are equal

Cubic polynomial equation (14) admits three equal roots provided the parameters satisfy the following two conditions,[56]

namely,

$$B^2 - 3AC = 0 \quad \text{and}$$
$$18ABCD - 4B^3D + B^2C^2 - 4AC^3 - 27A^2D^2 = 0. \tag{18}$$

Substituting the exact expressions of A, B, C, and D in (18) we end up at

$$\lambda_1 = \frac{-(k_1 + k_2)}{2} + i\frac{3\sqrt{3}}{2}\sqrt{a}\tau_1, \quad \tau_1 = \frac{|k_1 - k_2|}{\sqrt{a}}, \tag{19}$$

$$\tau_2 = \pm\frac{\tau_1}{\sqrt{ac - |b|^2}}. \tag{20}$$

The roots of (14) are given by $m_1 = m_2 = m_3 = -\frac{B}{3A} = -\frac{i}{3}(k_1 + k_2)$. Once the roots are determined, then one can follow the procedure given in the previous two cases and obtain the exact forms of first iterated solution $p[1]$ and $q[1]$. The resultant expressions
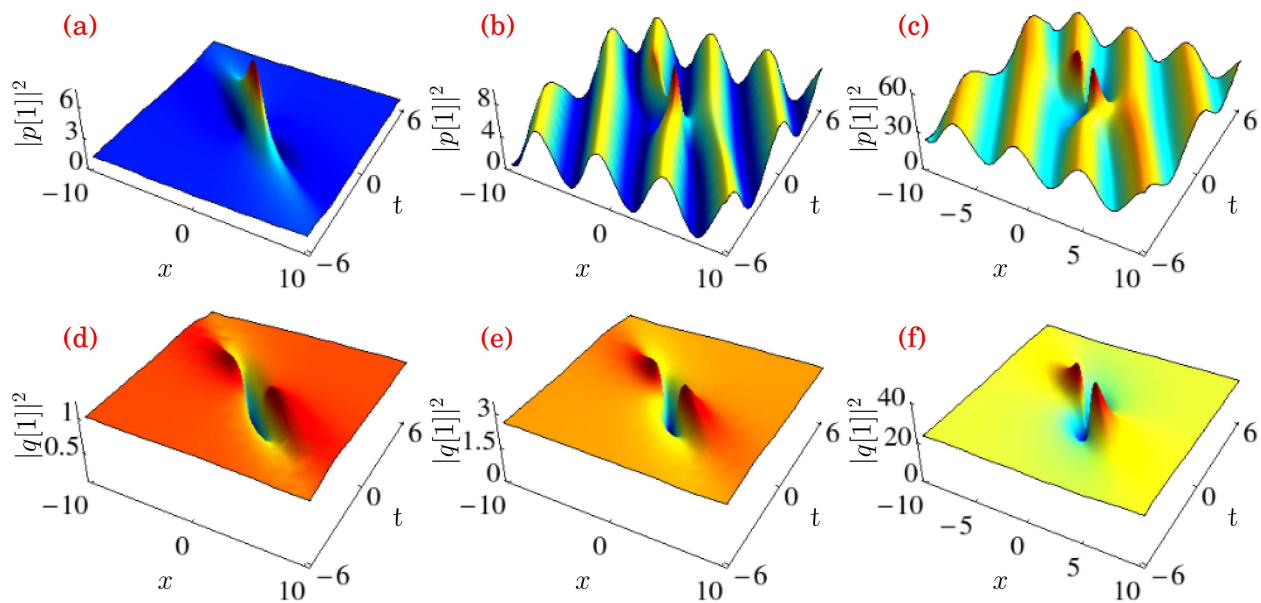
FIG. 5. (a) Rogue wave in $p[1]$ and (d) dark rogue wave in $q[1]$ for the parameter values $\lambda_1 = -0.276\,068 + 2.144\,98i$, $\tau_1 = 1$, $\tau_2 = 2$, $c_1 = 0$, $c_2 = 0$, $c_3 = 3$, $k_1 = -1$, $k_2 = 0.1$, $a = 0.5$, $c = 1.7$, and $b = 0.001 - 0.001i$. (b) Superposition of rogue wave on oscillating background in $p[1]$ and (e) four-petaled rogue wavelike form in $q[1]$ for the parameter values $\lambda_1 = -0.338\,411 + 2.815\,28i$, $a = 0.8$, $c = 1.4$, $b = 0.5 - 0.5i$, the other parameter values are as above. (c) Four-petaled rogue wave on oscillating background in $p[1]$ and (f) four-petaled rogue wave on constant background in $q[1]$ for the parameter values $\lambda_1 = -0.525\,693 + 5.917\,19i$, $a = 2.4$, $c = 3.49$, and $b = 2 - 2i$; the other parameter values are the same as above.

read

$$p[1] = \left(\left(1 + \frac{3\sqrt{3}a\tau_1 M_1}{1 + |\sqrt{a}\tau_1 M_1|^2 + |\sqrt{a\sigma}\tau_2 M_2|^2} \right) \tau_1 e^{ik_1 x + \omega_1 t} \right.$$

$$\left. - b^* \left(\left(1 + \frac{3\sqrt{3}a\tau_1 M_2}{1 + |\sqrt{a}\tau_1 M_1|^2 + |\sqrt{a\sigma}\tau_2 M_2|^2} \right) \tau_2 e^{ik_2 x + \omega_2 t} \right), \right.$$

$$q[1] = a \left(1 + \frac{3\sqrt{3}a\tau_1 M_2}{1 + |\sqrt{a}\tau_1 M_1|^2 + |\sqrt{a\sigma}\tau_2 M_2|^2} \right) \tau_2 e^{ik_2 x + \omega_2 t},$$
(21)

where M_1 and M_2 are given by

$$M_1 = \frac{2}{i(k_1 - k_2) - \sqrt{3}a\tau_1} + \frac{4}{(i(k_1 - k_2) - \sqrt{3}a\tau_1)^2} + \frac{R_1}{S},$$

$$M_2 = \frac{2}{i(k_2 - k_1) - \sqrt{3}a\tau_1} + \frac{4}{(i(k_2 - k_1) - \sqrt{3}a\tau_1)^2} + \frac{R_2}{S},$$

$$R_1 = \frac{2c_3}{(i(k_1 - k_2) - \sqrt{3}a\tau_1)^3} - \frac{2L}{(i(k_1 - k_2) - \sqrt{3}a\tau_1)^2},$$

$$R_2 = \frac{2c_3}{(i(k_2 - k_1) - \sqrt{3}a\tau_1)^3} - \frac{2L}{(i(k_2 - k_1) - \sqrt{3}a\tau_1)^2},$$

$$L = \frac{1}{2}c_3 x^2 + \frac{2}{9}(\lambda_1 - k_1 - k_2)^2 c_3 t^2$$

$$+ c_2 x + \frac{2}{3}(\lambda_1 - k_1 - k_2)c_2 t + ic_3 t$$

$$+ \frac{2}{3}(\lambda_1 - k_1 - k_2)c_3 xt + c_1,$$

$$S = \frac{1}{2}c_3 x^2 + \frac{2}{9}(\lambda_1 - k_1 - k_2)^2 c_3 t^2 + (c_2 + c_3)x$$

$$+ \frac{2}{3}(\lambda_1 - k_1 - k_2)(c_2 + c_3)t + ic_3 t$$

$$+ \frac{2}{3}(\lambda_1 - k_1 - k_2)c_3 xt + c_1 + c_2 + c_3.$$
(22)

The above solution is used to study the dynamics of vector rogue waves of CGNLS system (1).

### 1. The effect of four-wave mixing in case 3

To plot solution (21), first we should evaluate the exact value of λ_1 from expression (19) by substituting the other parameter values in it. Here also, we begin our studies by considering the case $b \to 0$. While plotting solution (21) with $b \to 0$, we visualize double rogue waves in both components. This result coincides with the
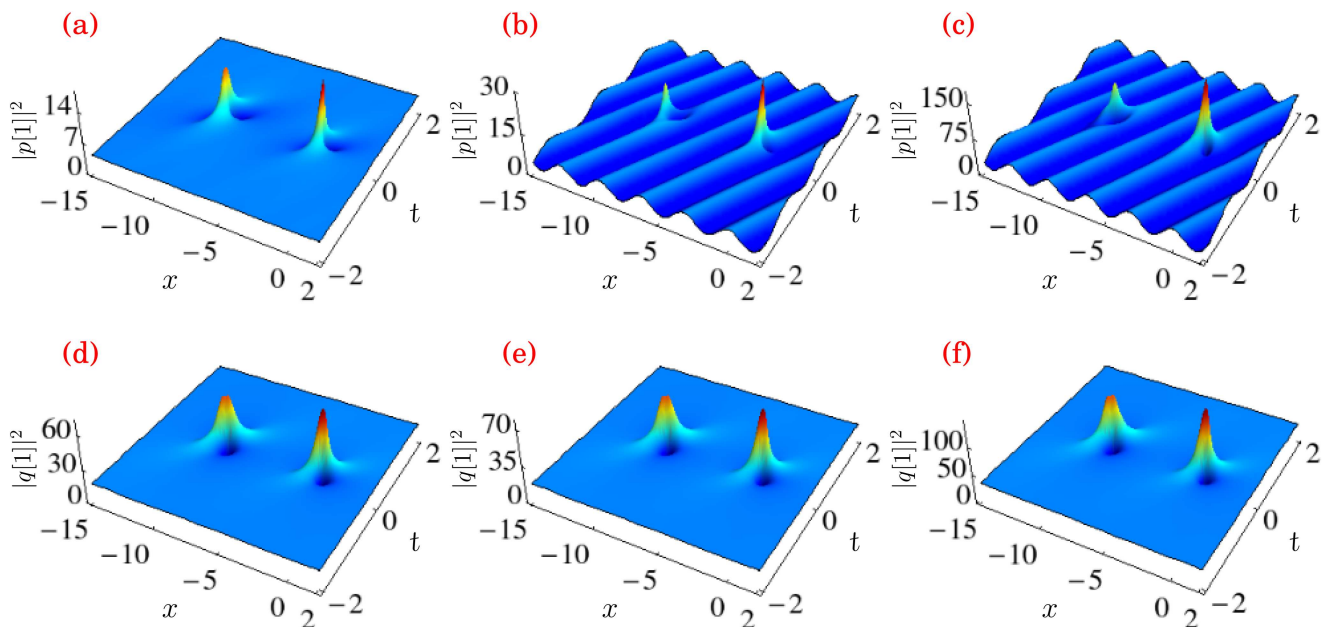
FIG. 6. (a) Double rogue wave in (a) the $p[1]$ component and (d) the $q[1]$ component for the parameter values $c_1 = 1$, $c_2 = 1$, $c_3 = 0.2$, $k_1 = 2.05$, $k_2 = 0.05$, $a = 1$, $c = 0.25$, and $b = 0.001 - 0.001i$. (b) Double rogue wave on oscillating background in $p[1]$ and (e) amplitude of double rogue wave increased in $q[1]$ for the parameter values $a = 1$, $c = 0.25$, and $b = 0.1 - 0.1i$; the other parameters are the same as above. (c) Amplitude of the double rogue wave increased on oscillating background in $p[1]$ and (e) amplitude of the double rogue wave increased in $q[1]$ for the parameter values $a = 1.7$, $c = 1.3$, $b = 1 - i$; the other parameters are the same as above.
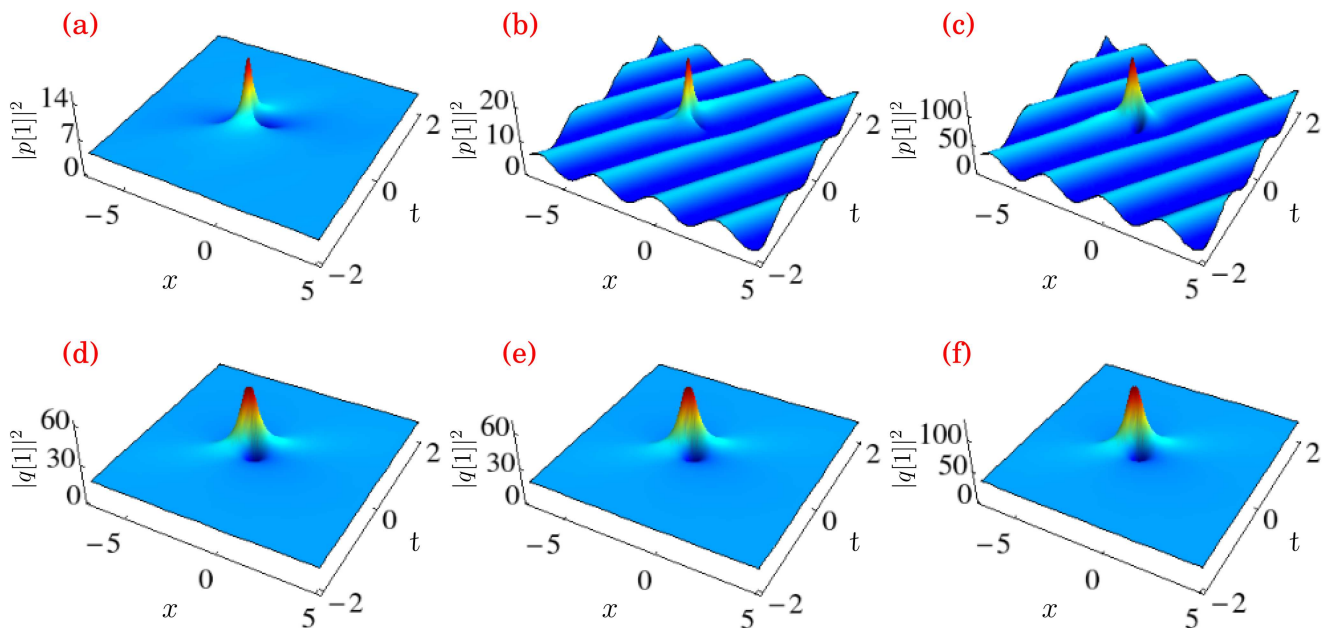
FIG. 7. (a) Single rogue wave in (a) the $p[1]$ component and (d) the $q[1]$ component for the parameter values $c_3 = 0$, the other parameters are as in Fig. 6. (b) Single rogue wave on oscillating background in $p[1]$ and (e) amplitude of single rogue wave increased in $q[1]$ for the parameter values $a = 1$, $c = 0.25$, $b = 0.1 - 0.1i$ and other parameter values are as above. (c) Amplitude of the single rogue wave increased on oscillating background in $p[1]$ and (e) amplitude of the single rogue wave increased in $q[1]$ for the parameter values $a = 1.7$, $c = 1.3$, $b = 1 - i$, the other parameter values are as above.
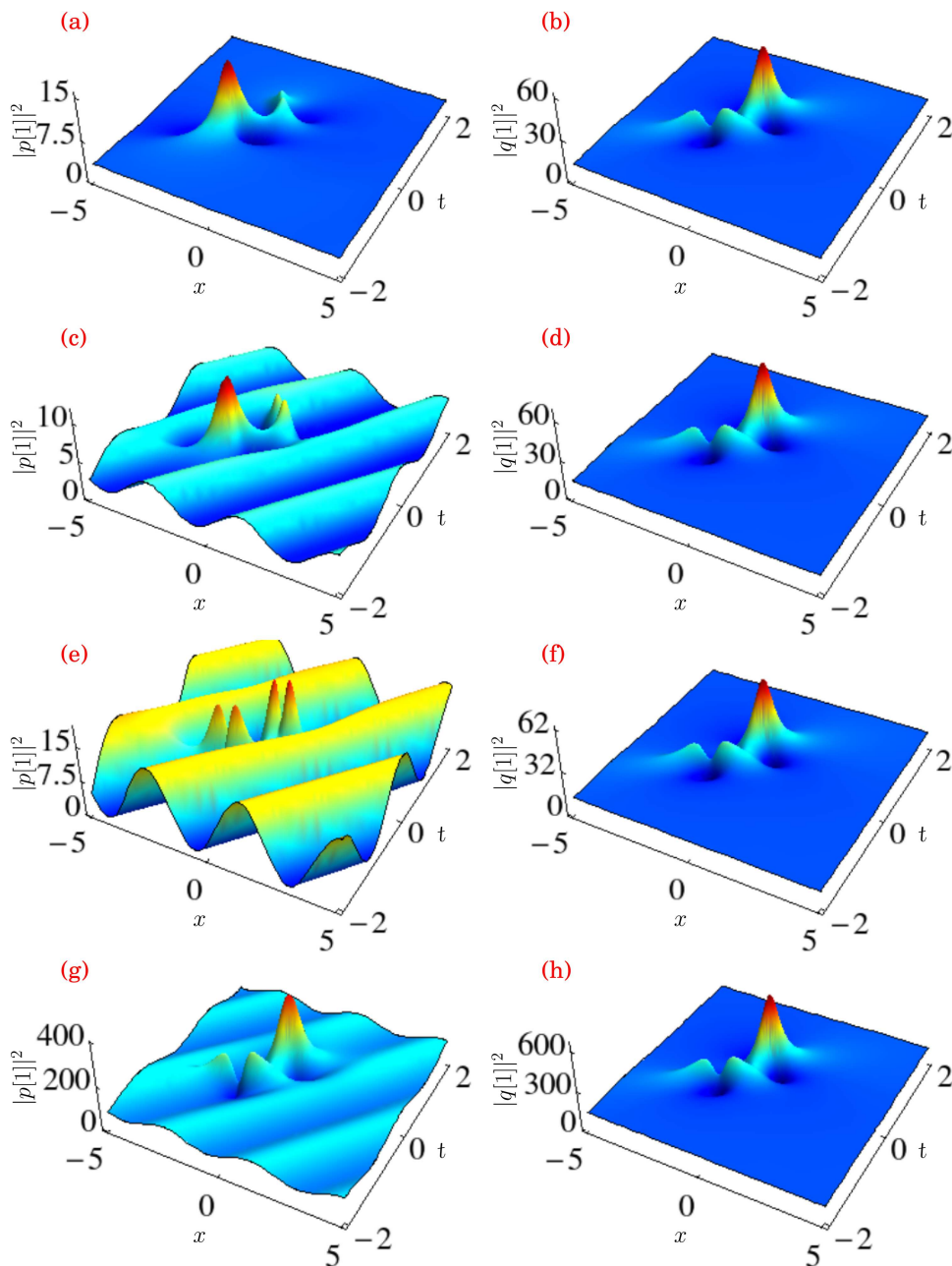
FIG. 8. Rogue wave with four-petaled rogue wave in (a) the $p[1]$ component and (e) the $q[1]$ component for the parameter values $c_1 = 0$, $c_2 = 0$, $c_3 = 0.2$, $k_1 = 1.75$, $k_2 = 0.05$, $a = 1$, $c = 0.25$, and $b = 0.001 - 0.001i$. Rogue wave with four-petaled rogue wave in (b) the $p[1]$ component on oscillating background and (f) the $q[1]$ component on constant background for the parameter value $b = 0.1 - 0.1i$; the other parameters are the same as above. (c) Two four-petaled rogue waves on oscillating background in $p[1]$ (g) amplitude of rogue wave increased in $q[1]$ for the parameter values $a = 1.1$, $c = 0.7$, and $b = 0.5 - 0.5i$; the other parameters are the same as above. (d) Four-petaled rogue transits to rogue wave and rogue wave transits to four-petaled rogue wave in $p[1]$ and (h) amplitude of rogue wave increased in $q[1]$ for the parameter values $a = 1.7$, $c = 1.2$, $b = 1 - i$; the other parameters are the same as above.

one reported in Ref. 28. When we increase the value of four-wave mixing parameter b to $0.1 + 0.1i$, these double rogue waves appear on oscillating background in the $p[1]$ component. The background density of $q[1]$ does not oscillate. One may note that the amplitude of these double rogue waves increases in both components $p[1]$ and $q[1]$ for higher values of b as shown in Fig. 6. For the choice $c_3 = 0$ and $b \to 0$, we come across only one rogue wave in both components [see Figs. 7(a) and 7(d)]. These figures reveal that the amplitude of rogue wave keeps on increasing for higher values of b.

Next, we move on to the case $M_1, M_2 \neq 0$ and $b \to 0$. For the choice $c_1 = c_2 = 0$, we visualize one rogue wave and one four-petaled rogue wave in both components as shown in Figs. 8(a) and 8(b). When we increase the value of b to $b = 0.1 - 0.1i$, the rogue wave appears on the oscillating background in the $p[1]$ component, whereas it appears on the constant background in the $q[1]$ component. When we increase the value of b further, we observe that the bright rogue wave becomes a four-petaled rogue wave and the four-petaled rogue wave becomes a rogue wave, which is illustrated

in remaining Fig. 8. The four-wave mixing effect transforms a rogue wave into a four-petaled rogue wave and a four-petaled rogue wave into a rogue wave. As far as the $q[1]$ component is concerned, we observe that the changes occur only in amplitudes, which, in turn, increase for higher values of b.

IV. CONCLUSIONS

In this paper, we have analyzed in detail the effect of four-wave mixing in the interactions among nonlinear waves such as solitons, breathers, and rogue waves of CGNLS system (1). Since this effect cannot be studied directly, we have transformed the CGNLS equation into the Manakov system in which we have constructed the plane wave solution with two different backgrounds. Once the desired solutions are obtained, we have transformed them into the original CGNLS variables. Our results reveal that the four-wave mixing parameter influences the nonlinear wave significantly. Our studies also show that the four-wave mixing parameter makes the following changes in the interaction picture between localized waves, namely, (i) the bright soliton takes a breather form, (ii) the number of pulses and the amplitude of the breather increases by increasing the values of the four-wave mixing parameter, and (iii) the depth of the dark soliton decreases for higher values of the four-wave mixing parameter. We have brought out several new interesting results, such as superposition of breather pulses, how the rogue wave and dark rogue wave become four-petaled rogue wave, existence of double rogue waves on an oscillating background, and how the rogue wave turns into a four-petaled rogue wave and the four-petaled rogue wave becomes a rogue wave. Another important result that we have observed is that the bright soliton becomes a dark oscillating soliton in a bright soliton-rogue wave interaction. Since dark solitons have many potential applications in fiber optics, we believe that our result will be useful in that area.[57] We also note that the aforementioned results have been brought out only by choosing two different background seed solutions for the components p and q.

In Ref. 58, the authors have proposed a novel technique to study the interaction between waves and ships/structures during extreme ocean conditions using breather solutions. In that reference, the authors pointed out that breathers can be exploited to generate rogue wave events for the systematic investigation of the impact on ships and these results will change the standards for building ships is a matter. We believe that studies on the increment in the number of breather pulses and amplitudes of breathers and rogue waves will have potential applications in these types of experiments. The various nonlinear wave solutions discussed in this paper, such as soliton, breather, and rogue wave, have also been realized in the context of both scalar and coupled NLS-type evolution equations representing wave propagation in optical fibers, Bose-Einstein condensates, plasma physics, oceanography, and so on. We expect that our results on the multicomponent CGNLS system can lead to the realization of the above type of coherent structures in multimode systems where four-wave mixing is important.

ACKNOWLEDGMENTS

REFERENCES

[1] G. Fibich, *The Nonlinear Schrödinger Equation: Singular Solutions and Optical Collapse* (Springer International Publishing, 2015).

[2] B. A. Balomed, "Nonlinear Schrödinger equation," in *Encyclopedia of Nonlinear Science*, edited by A. Scott (Routledge, London, 2005).

[3] S. Boscolo and C. Finot, *Shaping Light in Nonlinear Optical Fibers* (John Wiley & Sons Ltd, Chichester, 2017).

[4] G. P. Veldes, J. Borhanian, M. McKerr, V. Saxena, D. J. Fratzeskakis, and I. Kourakis, J. Opt. **15**, 064003 (2013).

[5] A. Chabchoub, N. Hoffmann, M. Onorato, and N. Akhmediev, Phys. Rev. X **2**, 011015 (2013).

[6] J. M. Dudely, F. Dias, M. Erkintalo, and G. Genty, Nat. Photonics **8**, 755 (2014).

[7] Y. V. Bludov, V. V. Konotop, and N. Akhmediev, Opt. Lett. **34**, 3015 (2009).

[8] K. Manikandan, P. Muruganandam, M. Senthilvelan, and M. Lakshmanan, Phys. Rev. E **90**, 062905 (2014).

[9] M. Onorato, S. Resitori, and F. Baronio, *Rogue and Shock Waves in Nonlinear Dispersive Media* (Springer, 2016).

[10] D. Mandelik, H. S. Eisenberg, Y. Silberberg, R. Morandotti, and J. S. Aitchison, Phys. Rev. Lett. **90**, 253902 (2003).

[11] Y. Tao and J. He, Phys. Rev. E **85**, 026601 (2012).

[12] S. Xu, J. He, and L. Wang, Europhys. Lett. **97**, 30007 (2012).

[13] S. Chen, Phys. Rev. E **88**, 023202 (2013).

[14] Y. Ohta and J. Yang, Phys. Rev. E **86**, 036604 (2012).

[15] A. Ankiewicz, J. M. Sotocrespo, M. Choudhury, and N. Akhmediev, J. Opt. Soc. Am. B **30**, 87 (2013).

[16] W. X. Li, Z. W. Guo, Z. B. Guo, and Z. H. Qiang, Commun. Theor. Phys. **58**, 531 (2012).

[17] X. Y. Wen, Y. Yang, and Z. Yan, Phys. Rev. E **92**, 012917 (2015).

[18] X. Y. Wen and D. S. Wang, Wave Motion **79**, 84 (2018).

[19] X. Y. Wen and Z. Yan, J. Math. Phys. **59**, 073511 (2018).

[20] S. V. Manakov, Sov. Phys. JETP **38**, 248 (1974).

[21] C. R. Menyuk, IEEE J. Q. Electron **23**, 174 (1987).

[22] Y. Kodama and A. V. Mikhailov, Physica D **152**, 171 (2001).

[23] O. C. Wright and M. G. Forest, Physica D **141**, 104 (2000).

[24] Q. H. Park and H. J. Shin, IEEE J. Sel. Top. Quantum Electron. **8**, 432 (2002).

[25] R. Radhakrishnan, M. Lakshmanan, and J. Hietarinta, Phys. Rev. E **56**, 2213 (1997).

[26] F. Baronio, A. Degasperis, M. Conforti, and S. Wabnitz, Phys. Rev. Lett. **109**, 044102 (2012).

[27] G. B. Ling and L. L. Ming, Chin. Phys. Lett. **28**, 110202 (2011).

[28] L. C. Zhao and L. Liu L, J. Opt. Soc. Am. B **29**, 3119 (2012).

[29] L. M. Ling, B. L. Guo, and L. C. Zhao, Phys. Rev. E **89**, 041201(R) (2014).

[30] L. C. Zhao, B. L. Guo, and L. M. Ling, J. Math. Phys. **57**, 043508 (2016).

[31] L. M. Ling, L. C. Zhao, and B. L. Guo, Commun. Nonlinear Sci. Numer. Simulat. **32**, 285 (2016).

[32] J. H. Li, H. N. Chan, K. S. Chiang, and K. W. Chow, Commun. Nonlinear Sci. Numer. Simulat. **28**, 28 (2015).

[33] S. Chen and D. Mihalache, J. Phys. A Math. Theor. **48**, 215202 (2015).

[34] G. Zhang, Z. Yan, X. Y. Wen, and Y. Chen, Phys. Rev. E **95**, 042201 (2017).

[35] R. Radha, P. S. Vinayagam, and K. Porsezian, Commun. Nonlinear Sci. Numer. Simulat. **37**, 354 (2016).

[36] Y. H. Qin, L. C. Zhao, Z. Y. Yang, and W. L. Yang, Chaos **28**, 013111 (2018).

[37] *Emergent Nonlinear Phenomena in Bose-Einstein Condensates: Theory and Experiment*, edited by P. G. Kevrekidis, D. J. Frantzeskakis, and R. C. González (Springer, Berlin, 2008).

[38] V. G. Makhankov and O. K. Pashaev, Theor. Math. Phys. **53**, 979 (1982).

[39] X. Lü and M. Peng, Nonlinear Dyn. **73**, 405 (2013).

[40] D. S. Wang, D. J. Zhang, and J. Yang, J. Math. Phys. **51**, 023510 (2010).

[41] N. Vishnu Priya and M. Senthilvelan, Commun. Nonlinear Sci. Numer. Simulat. **36**, 366 (2016).

[42] N. Vishnu Priya, M. Senthilvelan, and M. Lakshmanan, Phys. Rev. E **89**, 062901 (2014).

[43] N. Vishnu Priya and M. Senthilvelan, Phys. Scr. **90**, 025203 (2015).

[44] N. Vishnu Priya and M. Senthilvelan, Commun. Nonlinear Sci. Numer. Simul. **20**, 401 (2015).

[45] N. Vishnu Priya and M. Senthilvelan, Wave Motion **54**, 125 (2015).

[46] S. P. T. Mukam, V. K. Kuetche, and T. B. Bouetou, Eur. Phys. J. Plus **132**, 182 (2017).

[47] A. Agalarov, V. Zhulego, and T. Gadzhimuradov, Phys. Rev. E **91**, 042909 (2015).

[48] Y. Q. Yuan, B. Tian, L. Liu, and Y. Sun, Europhys. Lett. **120**, 30001 (2017).

[49] Y. Q. Yuan, B. Tian, H. P. Chai, X. Y. Wu, and Z. Du, Appl. Math. Lett. **87**, 50 (2019).

[50] Y. S. Kivshar and G. Agrawal, *Optical Solitons: From Fibers to Photonic Crystals* (Academic Press, London, 2003).

[51] D. M. Pepper, J. AuYeung, D. Fekete, and A. Yariv, Opt. Lett. **3**, 7 (1978).

[52] A. Yariv, *Quantum Electronics* (John Wiley & Sons, New York, 1989).

[53] H. J. Gerritsen, Appl. Phys. Lett. **10**, 239 (1967).

[54] T. Yajima and H. Souma, Phys. Rev. A **17**, 309 (1978).

[55] O. C. Wright, Appl. Math. Lett. **16**, 647 (2003).

[56] A. Jeffrey and D. Zwillenger, *Table of Integrals, Series and Products* (Academic Press, New York, 2007).

[57] W. Zhao and E. Bourkoff, Opt. Lett. **14**, 703 (1989).

[58] M. Onorato, D. Proment, G. Clauss, and M. Klein, PLoS One **8**, e54629 (2013).